DOE/ER/54445--1

Final Report for the Sept. 1997 - Jan. 2000 Period of
Contract No. DE-FG02-97ER54445
"Fundamental Science of High-density Fluorocarbon Plasmas"

G. S. Oehrlein (a)
Department of Physics, State University of New York at Albany
Albany, New York 12222

H. M. Anderson, and J. L. Cecchi
Department of Chemical and Nuclear Engineering, The University of New Mexico, Albuquerque, N.M.

(a) Current address: Department of Materials and Nuclear Engineering, University of Maryland, College Park, Md

SUMMARY

This report describes the results we obtained during the two and a half year of our work on the contract "Fundamental Science of High-Density Fluorocarbon Plasmas." In this program we established critical elements of the scientific knowledge base of high-density fluorocarbon plasmas used for SiO_2 patterning. To this end we characterized the species that exist in the gas phase and the processes that occur at relevant surfaces in contact with the plasma using complementary diagnostic instrumentation for plasma and surface characterization at two universities. By moving diagnostics from one university to the other, the full spectrum of diagnostics was applied to a single plasma reactor and fluorocarbon plasma etching process. The results of these measurements were correlated with data obtained when patterning SiO_2 using identical conditions. In parallel, a reactive beam scattering system was employed to establish the consequences of the interaction of mass- and energy-resolved low energy ions with SiO_2 and resist surfaces. Because of the move of one of the PI's (GSO) to the University of Maryland, College Park, this program terminated at the end of January 2000.

We initially summarize highlights of the progress that has been achieved. This is followed by a more extended description of selected items. A list of publications acknowledging support under this grant is presented at the end.

- We completed joint experiments for which an IR laser diode spectroscopy setup was moved from UNM to SUNY-Albany. During the course of these measurements absolute densities of CF, CF_2 and COF_2 were determined as a function of process parameters. These studies combined the principal gas phase and surface diagnostic techniques of this research effort and are a significant basis of our efforts to relate the fluxes of radical etchant species to the wafer, the surface characteristics of the wafer, the formation of etching profiles and evolution of etch products from the wafer in a quantitative model of this complex plasma chemistry process. These joint experiments yielded extensive data sets for several key fluorocarbon processing discharges (C_2F_6, CHF_3, and C_4F_8).
- We have measured the electron-impact dissociation rate for the C_2F_6 feedstock gas, and have determined how much of the carbon content of CHF_3 feedstock is contained in the two dominant precursors, CF and CF_2.
- We have also undertaken a comparison of two methods of measuring the concentrations of CF and CF_2, namely actinometry and diode-laser absorption spectroscopy.
- We correlated our gas phase concentration results with the rate of fluorocarbon film formation on the wafer. From these correlations, using a model derived previously, we are able to infer the sticking coefficients of CF and CF_2 during the formation of the protective film.
- By performing diode laser, gas phase measurements of radical etchant and reactant species formed in C_4F_8 discharges while etching oxide substrates at a high bias power, we were able to show that the concentrations

DISCLAIMER

DISCLAIMER

Portions of this document may be illegible in electronic image products. Images are produced from the best available original document.

of CF_2 and CF are reduced by 50% during etching of SiO_2 relative to conditions without ion bombardment. This indicates that CF_2 and CF are consumed during the etching of SiO_2.

- We measured fluorocarbon deposition and SiO_2 etching rates inside microstructures versus selfbias voltage (average ion energy) and as a function of microstructure dimensions. We established a model for the rate-limiting processes.
- By employing a weak magnetic field aligned with microstructures to selectively deflect electrons we were able to show that sidewall charging by incident electrons is the root cause of microtrenching seen during microfeature fabrication.
- We showed that the role of the fluorocarbon surface layers present on silicon during selective etching is to reduce the energy deposition into the substrate and mixing with etchant atoms, thus reducing the importance of ion-assisted etching.
- The fluorination of fluorocarbon plasma processed SiO_2 and Si_3N_4 samples for selective etching chemistries has been determined as a function of fluorocarbon overlayer thickness and is consistent with an etching model where the attack of fluorine atoms of the substrate is prevented by an increasing thickness of a steady-state overlayer.
- A low-energy ion source facility for ion-surface interaction studies with stable operation with fluorocarbon gases and reduced maintenance was established during this period. Clean beams of energy- and mass-resolved fluorocarbon ions can be produced with this system and were employed for low energy fluorocarbon ion bombardment of SiO_2 and resist surfaces. A significant difference between CF_3^+ and CF^+ ion bombardment of SiO_2 surfaces was established at an ion energy of 300 eV: While CF_3^+ ions induce SiO_2 etching, fluorocarbon film deposition is observed for CF^+ ion bombardment. We were unable to determine to what extent this difference was due to the unavoidable neutral background.

A. Plasma Studies

1. Measurement Of Reactive Species Concentrations

a. CF and CF_2 Concentration Measurements and Comparisons for Several Reactors

In sorting out the complex deposition and etching processes that occur at the interface between a substrate anda fluorocarbon plasma, it is imperative to know the gas phase concentrations of reactive species that are incident on the substrate. In the first phase of this work, we have studied how the concentrations of reactive species depend upon the plasma operating conditions.

Experiments were carried out using the inductively coupled plasma (ICP) chamber of the UNM plasma etch cluster tool. The ICP chamber includes a mechanically clamped chuck for 150 mm wafers, which are positioned 12 cm from the ICP quartz window. The primary diagnostic is a wavelength-modulated infrared diode laser absorption spectroscopy system used to measure the concentrations of CF_3, CF_2, and CF, which are the principle reactive species for the fluorocarbon plasmas studied here. Using an N_2O reference cell, the diode laser has been calibrated to provide absolute concentrations of the reactive species. Additional diagnostics include an optical multichannel analyzer (OMA) to measure emission from F and Ar, and a Langmuir probe to measure ion current to the wafer. A special cleaning procedure is followed to ensure that the probe remains clean, even in the presence of deposition due to the fluorocarbon plasma. Highlights of the measurements are as follows.

The rotational temperature of CF_2 was measured for a CHF_3/Ar (90:10) plasma at 15 mTorr over the ICP power range of 500 to 1500 W. Rotational lines J=10-24 of the ν_1 band $^RQ_8$ were used for analysis. The results indicate a rotational temperature of 529 +/- 24 K over the entire range of ICP power. Anticipating that the coupling between rotational and vibrational degrees of freedom will be high, this elevated rotational temperature likely reflects an increase in the reactivity of CF_2.

Measurements of reactive species concentrations were carried out for $C_2F_6/H_2/Ar$ (45%/45%/10%) fluorocarbon plasmas over the pressure range of 5 to 15 mTorr and for ICP powers for 300 to 1500 W (see Fig. 1). The concentration of CF_3 was below detectability ($< 5 \times 10^{10}$ cm^{-3}) over the entire experimental range. CF_2 decreases monotonically with ICP power for 5 and 10 mTorr. For 15 mTorr, CF_2, peaks at 400 W, and then decreases for higher powers. The maximum CF_2 concentration, which occurs at 15 mTorr and 400 W, is 1.2×10^{14} cm^{-3}, which is approximately equivalent to a partial pressure of 4 mTorr, assuming room temperature translational energy. The concentration of CF increases monotonically with ICP power and pressure. The maximum concentration, which occurs at 15 mTorr and 1500 W, is 1×10^{14} cm^{-3}, which is approximately equivalent to a 3.3 mTorr partial pressure. The ratio $[CF_2]/[CF]$ varies from approximately 8 at low powers to 0.5 at the highest powers.

Reactive species concentrations were also measured for $CHF_3/C_2HF_5/Ar$ (30%/60%/10%) fluorocarbon plasmas at 10 and 30 mTorr up to 2500 W of ICP power. CF_3 was below the detectable limit. CF_2 attained a maximum concentration of 1×10^{15} cm^{-3} at 1000 W and 30 mTorr. This is equivalent to a partial pressure of approximately 33 mTorr, which is slightly greater than the starting pressure, although a direct comparison is not really appropriate, since the feedstock contains a large fraction of di-carbon molecules. Nevertheless, it is apparent that for this feedstock combination at higher pressures like 30 mTorr, there is a very large concentration of CF_2 for low powers. CF_2 decreases with ICP power above this maximum. CF increases monotonically with ICP power, exhibiting only a small increase in going from 10 to 30 mTorr. The maximum concentration of CF occurs at 30 mTorr and 2500 W, and is 1.6×10^{14} cm^{-3}, only slightly greater than for the $C_2F_6/H_2/Ar$, even though the pressure is considerably higher. At 30 mTorr, the $[CF_2]/[CF]$ ratio varies from approximately 20 down to 4 at 2500 W. The ratio is less for the 10 mTorr case and is similar to the ratio for the 10 mTorr case of $C_2F_6/H_2/Ar$.

The diode laser-based gas phase measurements of radical etchant and reactant species were extended to C_2F_6, CHF_3 and C_4F_8 discharges while etching oxide substrates. These measurements were made on the Gaseous Electronics Conference (GEC), inductively coupled plasma (ICP) Reference Cell at UNM, the ICP chamber of the UNM plasma etch cluster tool, and the SUNY-Albany ICP reactor/surface analysis tool. The latter experiments took place after the diode laser of UNM's Professor Harold Anderson was transported to Albany and installed on the SUNY-Albany reactor. These collaborative measurements effort brought together UNM's expertise in infrared diode laser spectroscopy with the SUNY Albany expertise on *in situ* etch rate measurements, surface characterization, and spatially resolved mass spectrometry. The goal of this work was to correlate radical densities with microstructure etching and surface characterization work on Si, SiO_2, Si_3N_4, and photoresist thin films undergoing etching, all being performed in the same reactor. Moreover, the comparison of data obtained in three different reactors provides an assessment on the applicability of particular data sets to other reactors. Absolute densities of the various radical and etch product species observed in the discharge are made based on the linestrength formula. The diode laser experiments at both UNM and SUNY-Albany focused on correlating etchant and reactant species concentrations found in the discharge in reactor operating parameter space typical of commercial high density plasma oxide etching, and have provided significant new insight into the mechanism and kinetics of oxide etching in high density ICP reactors.

As an example, we shown in Figure 1 the source power and pressure dependence of the CF and CF_2 number density observed in CHF_3 discharges in the SUNY-Albany reactor. Equivalent measurements were also performed for C_2F_6 and C_4F_8 discharges but are not shown. Briefly, for C_2F_6 discharges, the behavior of CF and CF_2 is similar to that observed in the GEC/ICP Cell, but the concentrations are lower by about a factor of two. This most likely is due to a greater capacitive coupling component in the SUNY-Albany reactor. However, on switching gases to CHF_3 or C_4F_8, the concentrations of both CF and CF_2 are significantly greater than those observed in the GEC/ICP Cell with C_2F_6. This clearly must be related to distinctly different chemical reactions occuring in the discharge and/or the reactor wall.

b. Time Evolution Of Fluorocarbon Radical Concentrations During Pulsed Oxide Etching Plasmas In An ICP Reactor

We have measured the time evolution of the concentrations of the fluorocarbon radical precursors, CF_2 and CF, in pulsed plasmas using oxide etching chemistries. These measurements were performed in an inductively coupled plasma (ICP) reactor with CHF_3/Ar and CHF_3/H_2 feeds. We have explored a range of ICP powers of 300 to 900 W and a range of total pressure from 10 to 100 mTorr. The concentrations of CF_2 and CF were measured with a wavelength-modulated diode laser spectroscopy system, modified to provide data with a time resolution of less than 0.3 ms. The pulse repetition rate and duty factor were varied to explore a large range of CF_2 and CF kinetics. Following the initiation of the plasma, [CF] increases in a nearly first-order manner. The time behavior of [CF] during the plasma on time is not consistent with CF being formed by electron-impact dissociation of CF_2. The behavior of $[CF_2]$ is more complicated. Under pulsing conditions where $[CF_2]$ remains nonzero for the entire period, there is an initial, very rapid (< 3 ms) decrease in $[CF_2]$, indicating an enhanced loss, followed by a slower rise to equilibrium. After the termination of the plasma, $[CF_2]$ shows a rapid increase and a slower increase, followed by an exponential decay. Under some conditions, [CF] increases slightly after termination of the plasma. The [CF] decay is very close to first order in all cases. The time constant for $[CF_2]$ decay is in the range of 0.08-0.20 s, while the time constants for [CF] are more than a factor of ten smaller. Both time constants decrease with increasing pressure, and show a much smaller dependence on ICP power.

c. Carbon Mole Balance

Previous measurements have determined that CF and CF_2 are the dominant precursors during selective oxide etching with fluorocarbon feedstocks. It is of interest to compare the total carbon concentration of these precursors with the initial carbon concentration in the feedstock. We have investigated this in the ICP chamber of the UNM cluster etch tool for CHF_3 at ICP powers from 500 to 1500 W and pressures of 5 to 30 mTorr. We have used the diode laser system to measure the CF and CF_2 absolute concentrations. In Figure 2, we plot the ratio of $[CF] + [CF_2]$ to $[CHF_3]$ over the entire parameter range. At the two highest pressures, the ratio varies from about 0.4 at 500 W down to about 0.3 at 1500 W. For the 5 mTorr case, the ratio is considerably lower.

It is important to note that we do not expect the ratio to be unity. The concentration, N is given by

$$N = \Gamma\tau/V, \qquad (1)$$

where Γ is the molar flow rate, τ is the residence time and V is the reactor volume. Given the high probability for CF and CF_2 to stick to surfaces, we expect their respective residence times to be smaller than that of CHF_3, which would tend to make the ratio less than unity. The fact that the ratio is as close to unity as indicated in Figure 2 does suggest that most of the carbon in the CHF_3 discharge is in CF and CF_2.

d. COF_2 Etch Product Identification and Quantification

Several new absorption peaks were discovered in the 1230 to 1231 cm^{-1} range of the IR spectrum during O_2-based chamber cleaning. These peaks were also found to be present in fluorocarbon discharges in the SUNY-Albany reactor when the degree of capacitive coupling of the coil at the quartz window is significant (see Fig. 3). These new absorption features were identified as being the etch product COF_2 . This was determined by matching absorption features of the previously unknown species formed in discharge with those due to a chamber backfill of pure COF_2 gas. We also characterized the behavior of the COF_2 etch product as a function of gas and reactor conditions. We observed that in C_2F_6 and C_4F_8, the concentration of COF2 is higher than that found in CHF_3 and there is a strong source power dependence of the COF_2 density. The difficulty in analyzing this response will be

in separating the COF_2 formed from etching of the oxide wafer versus that formed from plasma interaction with any quartz wall material. Clearly, there is a connection with the degree of capacitive coupling that occurs in the reactor which can influence the generation of this product.

e. Demonstration of the Consumption of CF_2 and CF During Etching of SiO_2

By performing diode laser, gas phase measurements of radical etchant and reactant species formed in C_4F_8 discharges while etching oxide substrates at a high bias power, major progress has been made during this period on the role of CF_2 and CF for the etching of SiO_2. The goal of diagnostics for plasma modeling at the University of New Mexico (UNM) in 2000 was to generate a sufficient data base to allow development of a plasma model for predicting oxide, photoresist (PR) and PR-patterned low dielectric constant, porous silica etch rates and uniformity in C_4F_8 plasmas. Diode laser spectroscopy (DLAS), OES and Langmuir probe measurements made in the Gaseous Electroncis Conference (GEC)-Inductively Coupled Plasma (ICP) Reference Cell while performing these etch experiments now provide a reasonably complete model for the C_4F_8 oxide etch process.

DLAS has shown that C_4F_8 is largely dissociated to form C_2F_4, CF_2 and CF in the discharge. Over an oxide surface, CF_2 and CF are consumed in the oxide etch process, but only when the bias power is sufficient to keep the oxide surface clean through energetic ion bombardment. Langmuir probe measurement of the ion current density was used to estimate the bias voltage at the wafer at which this transition took place. For C_4F_8, this transition occurs at ~ 60 eV (75 W bias power) in the GEC Cell. At higher bias powers (125 W) where oxide etching is fast (~600 nm/min.), CF_2 appears to be the key radical for the etch process since ~50 percent (2.7-3.0 mTorr in a 15 mTorr C_4F_8 discharge) is consumed. These values were obtained by comparing the CF_2 concentrations over non-reactive wafer surfaces versus blanket oxide wafer surfaces undergoing etching. CF is shown to display a similar trend, but its concentration is an order of magnitude less than CF_2, and consequently cannot account on a mass basis for the amount of reactants necessary to balance the amount of etch products. Over a PR surface, neither CF_2 nor CF concentrations vary as a function of PR etch rate. Consequently, they do not appear to be involved in the PR etch mechanism. However, PR etching is also critically dependent on bias power. PR films etch presumably due to energetic ion bombardment that degrades the PR film, making it liable to attack by fluorine. Patterned low-k (k=1.3-2.3) porous silica films prepared by Sol-Gel were also etched in GEC Reference Cell in C_4F_8. The as-made porous silica films exhibited a much higher bias power threshold for net etching over deposition compared to bulk oxide films. FTIR and XPS analysis of the porous silica established that in the as-made material there was a significant hydroxyl residue associated with the surface of the pore voids. Etching of this type of as-made, patterned porous silica exhibited premature etch stop and aspect ratio-dependent etch rate (ARDE) in C_4F_8 even at relatively large feature sizes. However, if the porous silica is given a fluorination pretreatment prior to etching to replace the hydroxyl groups with atomic fluorine, the etch behavior returns to being comparable to that of bulk oxide.

2. Surface Diagnostics, Microstructure Etching and Processes

a. Measurement Of The Sticking Coefficents For CF And CF_2

In previous work, we have shown that the rate of polymer deposition, DR, during selective oxide etching with a fluorocarbon plasma can be expressed as,

$$DR = k_1[CF] + k_{2l}[CF_2]I, \qquad (2)$$

where, [CF] and $[CF_2]$ are the concentrations of CF and CF_2 respectively, I is the ion current to the wafer, and k_1 and k_{2l} are kinetic parameters which we have measured empirically and to found to be constant over the power range of 200 to 200 W, pressure range of 5 to 15 mTorr, and for a variety of feedstocks, including CHF_3 and C_2F_6.

In Figure 4, we show a comparison of the incident flux of CF and the deposition rate that can be attributed to CF using the model in (2). The incident flux, Γ_{inc}, is given by

$$\Gamma_{inc} = [CF]v/4,$$

where v is the thermal velocity of CF. We define the "deposition flux", Γ_{dep}, as

$$\Gamma_{dep} = DR(CF)\, n_{film},$$

where DR(CF) is the deposition rate we calculate from the first term in (2) using the measured value of [CF] (determined from the diode laser) and n_{film} is the density of the polymer film. From the ratio of the incident CF flux to the deposition flux, we get that the sticking coefficient is 0.4. Following a similar procedure for CF_2, we find that the sticking coefficient varies from 0.01 to 0.07.

b. Role of Fluorocarbon Surface Film in Selective Etching

The CF_2 and CF fluorocarbon precursors strike surfaces and produce fluorocarbon films. For steady-state etching of SiO_2, silicon and resist films to take place, these fluorocarbon species need to be removed again to prevent net film growth. The balance between fluorocarbon film deposition and etching produces a thin steady-state fluorocarbon film on the surface, through which the etching of the substrate occurs. If the steady-state fluorocarbon layer becomes sufficiently thick, the etching rate of the substrate becomes surface-limited, rather than limited by the incident fluxes of ionic and neutral etchant species. Selective etching of SiO_2 relative to silicon and resist is possible when these films form on silicon and resist, but not SiO_2. Using the SUNY Albany plasma reactor/surface analysis cluster tool, we have employed real-time ellipsometry and x-ray photoemission spectroscopy upon transfer of etched samples in vacuum into a surface analysis system to study surface etching mechanism in inductively-coupled high-density plasmas. Etching rates and steady-state fluorocarbon film thicknesses for silicon, and ion currents for C_2F_6 discharges were measured by ellipsometry and Langmuir probe analysis, respectively. The operating pressure of the C_2F_6 discharge was varied from 6 to 20 mTorr, the total gas flow ranged from 10 to 40 sccm, and the inductive power level was adjusted from 600 to 1400W. The RF bias power was varied to maintain a constant selfbias voltage of -100 V for all conditions. Similar measurements were also undertaken for CHF_3 discharges.

Figure 5 (a) shows measured Si etch rates for a set of experiments as a function of fluorocarbon film thickness. A general trend of decreasing etch rate with increasing fluorocarbon film thickness is observed, but there is a great deal of scatter, especially for small fluorocarbon film thickness, and the silicon etch rate does no correlate in a unique fashion with the fluorocarbon film thickness. Since the ion density varies significantly across the investigated parameter space, it is more instructive to examine etch yields, i.e. number of substrate atoms removed per incident ion, as a function of fluorocarbon film thickness. Figure 5 (b) shows that the silicon etch yield decreases exponentially with fluorocarbon film thickness. We observe a universal relationship between silicon etch yield and fluorocarbon film thickness that describes all data taken under widely differing conditions. For a clean Si surface, the Si etch yield is about 1.5 Si atoms removed per incident ion.

Monte Carlo simulations of the stopping of ions in fluorocarbon films were performed. A possible interpretion of Fig. 5 (b) that is consistent with these simulations is that the ion energy loss that occurs within the first 1-2 nm of the steady-state fluorocarbon layer is the major factor in the reduction of the Si etch rate. As the fluorocarbon film grows to a thickness that exceeds 1 nm, the lack of direct ion bombardment and energy deposition into the Si substrate reduces the importance of ion-assisted etching. Ultimately, Si etching only occurs by direct spontaneous reaction with fluorine atoms that have migrated through the fluorocarbon film.

It is known that significant etching of SiO_2 in fluorocarbon gases without ion bombardment is not possible. This mechanism therefore also explains why for SiO_2 a steady-state fluorocarbon layer thickness of about 2 nm will produce etch stop.

c. Microstructure Etching

When fabricating microscopic features in SiO_2 layers using low pressure, high-density fluorocarbon plasmas, electron-induced charging of microstructure sidewalls has been suggested to be important. The reason for the

differential charging of different surface portions of the microstructure is the dissimilarity in the angular distribution of ion (directional, because of acceleration in the sheath) and electron velocities (isotropic, since electrons can only reach the wafer surface when the sheath fields disappear once per RF cycle). If differential charging were important, it would lead to deflection of positive ions to the feature sidewalls. This reduction of positive ion bombardment could limit our ability to produce high-aspect ratio features in insulating films.

During formation of trenches and vias in SiO_2, microtrenching has commonly been observed. Microtrenching has been explained as being either due to ion scattering from sloped sidewalls or deflection of ions by the negative charge on the feature sidewalls. We have used microtrenching as a diagnostic technique to show for the first time directly that electron-induced charging is responsible for ion deflection in these processes, rather than ion scattering from the mask or sidewalls. By using a weak magnetic field (about 100 Gauss) the electron motion in the microstructure can be affected, whereas the ion trajectories are not influenced by the magnetic field. Moreover, the direction for the magnetic-field induced deflection is different for electrons than for ions and the root cause of microtrenching can thus be identified. In our work, the application of a weak magnetic field produces a significant asymmetry in microtrenching, with a dependence on geometry that is precisely consistent with electron-based sidewall charging. Differential charging of microstructures is therefore an important issue that needs to be considered in the modeling and design of high-resolution patterning processes in insulating layers.

d. Fluorocarbon Deposition and SiO_2 Etching in Microstructures

Etching and deposition processes are expected to be strongly modified inside microstructures due to geometrical shadowing of neutrals and charging related effects that will modifiy the ion fluxes to the bottom of features. Figure 6 shows SiO_2 etch rates as a function of RF bias measured for various aspect ratios in a 40 sccm CHF_3 plasma at 1400W inductive power and 6 mTorr operating pressure. Similar to etching of blanket SiO_2 surfaces, a transition from fluorocarbon deposition at low RF bias to SiO_2 etching at high RF bias occurs in features. The current data show that the fluorocarbon deposition rate for a floating substrate decreases rapidly in the low aspect ratio regime (0.8 - 2). This decrease can be partly explained by a decrease of the neutral flux arriving at the feature bottom. In features with an aspect ratio larger than 2, no significant fluorocarbon deposition was observed at the feature bottom. Interestingly, in the aspect ratio range where the fluorocarbon deposition at the feature bottom shows significant changes, the SiO_2 etching rate at high RF bias does not show any significant aspect ratio dependence. In the high aspect ratio range (AR >2), where the fluorocarbon deposition is near zero, the SiO_2 etch rate shows a decrease with increasing aspect ratio. This decrease in SiO_2 etching rate should result from a reduction of the ion and/or energy fluxes to the bottom of features with increasing aspect ratio, e.g. due to differential charging effects.

e. Surface Analysis of Si_3N_4 and SiO_2 Surfaces for Selective Etching Processes

Achieving etching selectivity of SiO_2 or other insulators relative to Si_3N_4 is an important problem since Si_3N_4 is often employed as an etch stop layer. During fluorocarbon plasma etching, surfaces are typically covered by a thin fluorocarbon passivation layer through which the etching needs to occur. When performing X-ray photoelectron spectroscopy surface analysis on fluorocarbon plasma etched samples one finds that the C (1s) spectra (BE≈ 285 eV) can be deconvolved into four different Gaussian peaks corresponding to different chemical carbon bonds (C-CF_n, C-F, C-F_2, and C-F_3), which allows to determine the average fluorine to carbon ratio F/C_{dec} of the fluorocarbon passivation film

$$F / C_{dec} = \frac{I_{C-F} + 2 \cdot I_{C-F2} + 3 \cdot I_{C-F3}}{I_{C-C/C-Si/C-CFn} + I_{C-F} + I_{C-F2} + I_{C-F3}}, \qquad (3)$$

with I_{bond} the photoemission intensity originating from a specific bond. The fluorine-to-carbon ratio $F(1s)/C(1s)$ can also be calculated by dividing the intensity of the F (1s) spectrum (BE=687.1 eV) by the total C (1s) intensity, after correcting for differences in photoemission cross sections. Figure 7 shows the difference $\Delta F/C$ between the fluorine-to-carbon ratios determined by the two methods, i.e.:

$$\Delta F/C = F(1s)/C(1s) - F/C_{dec}, \qquad (4)$$

for both processed SiO_2 and Si_3N_4 surfaces as a function of fluorocarbon film thickness. The XPS analysis was performed at both 15^0 and 90^0 photoelectron take off angle. For XPS spectra obtained under 15^0 photoelectron take off angle, which is a surface sensitive condition, $\Delta F/C$ is close to zero. At 90^0 photoelectron take off angle $\Delta F/C$ is also close to zero at conditions where a relatively thick fluorocarbon film is present on the substrates. This data shows that the F (1s) photoelectrons detected from all samples using the 15^0 take off angle as well as from samples with a relatively thick fluorocarbon film on the surface using the 90^0 take off angle primarily originate from fluorine bonded to carbon in the fluorocarbon film. If the fluorocarbon film thickness is small, however, the $F(1s)/C(1s)$ ratio is found to be higher than the F/C_{dec} ratio, resulting in a value for $\Delta F/C$ that is larger than zero. This means that a significant part of the F (1s) photoelectrons detected from samples with a thin fluorocarbon film on the surface at 90^0 take off angle must originate from fluorine species that are not bonded to carbon. The fluorine that is not bonded to carbon, is found to be located underneath the fluorocarbon film in fluorinated SiO_2 and Si_3N_4 reaction layers. For instance, we find that the N(1s) spectra obtained with processed Si_3N_4 samples show two peaks. The low binding energy peak corresponds to N (1s) in bulk Si_3N_4 (BE = 397.5 eV). The high binding energy peak is shifted by 2.27 ± 0.35 eV and can be attributed to substrate nitrogen bonded to fluorine. A similar observation was made for the Si (2p) spectra obtained from the same samples. The formation of fluorinated Si and N is a prerequisite of Si_3N_4 etching and should be suppressed for SiO_2/Si_3N_4 selective etching conditions. The intensity ratio $I_{reacted}/I_{bulk}$ has been found to decrease with fluorocarbon film thickness, indicating that the transport of fluorinated etchants through the fluorocarbon film is the etch rate limiting factor (as opposed to out-diffusion of reaction products).

B. Reactive Beam Studies

1. Quantitative Etch Yield Measurements at Low Ion Energies

An apparatus called Plasma Understanding Simulation System (PLUSS) was used for the experimental simulation of plasma-surface interactions and employs mass and energy-selected ions with kinetic energy in the range 20 to 300 eV. Ions are extracted from a microwave plasma, mass-selected using a Wien filter and subsequently decelerated to the energies of interest. The erosion rates of thin film materials are measured using a quartz crystal microbalance (QCM) overcoated with the films of interest. One focus of the work was to develop procedures and corrections required for obtaining quantitative etch yield data for low energy ion etching experiments. We chose Ar+ ion etching of silicon dioxide as a benchmark, since the results of these interactions can be calculated by TRansport of Ions in Matter (TRIM) simulations. The spot size of low energy (<100 eV) ion beams depends strongly on ion energy, and the QCM sensitivity varies radially. A special sample holder with an aperture is used to defined the etching area. The profile of ion beam is monitored by a multi-ring setup. A calibration method of the QCM for the focused ion beam etching was developed based on the measured QCM sensitivity as a function of ion beam position, and the procedures for measurement of etch yield of beam etching by QCM was carried out. Quantitative etch yields of resist and SiO_2 by Ar ion beam etching were obtained using these procedures. We find that our SiO_2 etch yield data quantitatively agree with the results of TRIM simulations. The energy threshold of SiO2 etching is also consistent with the TRIM simulations, and similar to the threshold seen for resist etching.

2. New Fluorocarbon Ion Source

We also modified the ion source of the PLUSS system for continuous operation with reactive fluorocarbon gases. In the current configuration a microwave antenna is separated from the plasma by a quartz tube and produces an electron cyclotron resonance (ECR) plasma down to pressures of $8x10^{-6}$ mbar. Tests using CF4 discharges have shown that we are able to produce stable beams of mass resolved fluorocarbon ions. One problem that had to be addressed was the erosion of the quartz coupling tube by the ECR discharge. This produced SiF_2^+ ions (66 amu),

and COF^+ and SiF^+ ions (47 amu) which were superimposed on the fluorocarbon CF_3^+ (69 amu) and CF_2^+ (50 amu) ions. Use of an alumina liner eliminated all peaks due to SiFx species and enabled us to obtain a clean CFx ion spectrum is obtained. This is shown in Figure 8. For our operating conditions, CF^+ is the dominant ion. Initial experiments using 300 eV CF_3^+ and CF^+ ion bombardment of SiO_2 surfaces has established a significant difference in the response of SiO_2 to the bombardment by these ions. While CF_3^+ ions induce SiO_2 etching, fluorocarbon film deposition is observed for CF^+ ion bombardment (both at 300 eV).

Publications Acknowledging Support Under This Contract:

1. M. Schaepkens and G. S. Oehrlein, *"Asymmetric microtrenching during ICP oxide etching in the presence of a weak magnetic field"*, Appl. Phys. Lett. **72,** 1293 (1998).
2. M. Schaepkens, G. S. Oehrlein, Ch. Hedlund, L. B. Jonsson, and H.-O. Blom, *Differences in angular dependence of silicon dioxide and silicon nitride etching rates in an an inductively coupled fluorocarbon plasma*, J. Vac. Sci. & Technol. **A16,** 3281 (1998).
3. M. Schaepkens, T.E.F.M. Standaert, N.R. Rueger, P.G.M. Sebel, and G.S. Oehrlein, *Study of the SiO_2-to-Si_3N_4 etch selectivity mechanism in inductively coupled fluorocarbon plasmas and a comparison with the SiO_2-to-Si mechanism*, J. Vac. Sci. & Technol. **A17,** 26 (1999).
4. G. S. Oehrlein, M. F. Doemling, B. E. E. Kastenmeier, P. J. Matsuo, N. R. Rueger, M. Schaepkens, and T.E.F.M. Standaert, *Surface Science Issues in Plasma Etching*, IBM J. Res. & Develop. **43,** 181 (1999).
5. M. Schaepkens, G.S. Oehrlein, K. G. Donohoe, and J. M. Cook, *Effect of RF bias power on SiO_2 feature etching in inductively coupled fluorocarbon plasmas*, J. Vac. Sci. & Technol. **B 18**, 848 (2000).
6. M. Schaepkens, G.S. Oehrlein, K. G. Donohoe, and J. M. Cook, *Effect of RF bias frequency and RF bias pulsing on SiO_2 feature etching in inductively coupled fluorocarbon plasmas*, J. Vac. Sci. & Technol. **B 18**, 856 (2000
7. M. Schaepkens, N. R. Rueger, J. J. Beulens, X. Li. T. E. F. M. Standaert, P. J. Matsuo, and G. S. Oehrlein, *The Effect of Capacitive Coupling on Inductively Coupled Fluorocarbon Plasma Processing*, J. Vac. Sci. & Technol. **A 17**, 3272 (1999).
8. M.J. Sowa, M.E. Littau, V. Pohray, and J.L. Cecchi, *Fluorocarbon Polymer Deposition Kinetics in a Low-Pressure High-Density Inductively Coupled Plasma Reactor*, J. Vac. Sci. Technol. **A 18**, (2000) 2122.
9. M. F. Doemling, B. Lin, N. R. Rueger, G. S. Oehrlein, and R. A. Haring, *Using a Quartz Crystal Microbalance (QCM) for Low Energy Ion Beam Etching Studies*, J. Vac. Sci. & Technol. **A 18,** 232 (2000).
10. W.L. Perry, K. Waters, M. Barela, G. Van Ullen and H.M. Anderson, *Oxide Etch Behavior in a High-Density, Low-Pressure, Inductively-Coupled C2F6 Plasma: Etch Rates, Selectivity to Photoresist, Plasma Parameters and CFx Radical Densities*, in press, JVST B (2001).
11. M. Schaepkens, I. Martini, E.A. Sanjuan, X. Li, G.S. Oehrlein, W.L. Perry and H.M. Anderson *Gas-Phase Studies in Inductively Coupled Fluorocarbon Plasmas*, (submitted for publication, J. Vac. Sci. Technol. A).
12. M. Schaepkens and G. S. Oehrlein, *A Review of SiO2 Etching in Inductively Coupled Fluorocarbon Plasmas*, Journal of Electrocemical Society 148 (3), page xx (2001).
13. M.E. Littau, M.J. Sowa, and J.L. Cecchi, *Diode Laser Measurements of CFx Species in a Low-Pressure High-Density Plasma Reactor*, (Submitted for publication, J. Vac. Sci. Technol. A).

Figures:

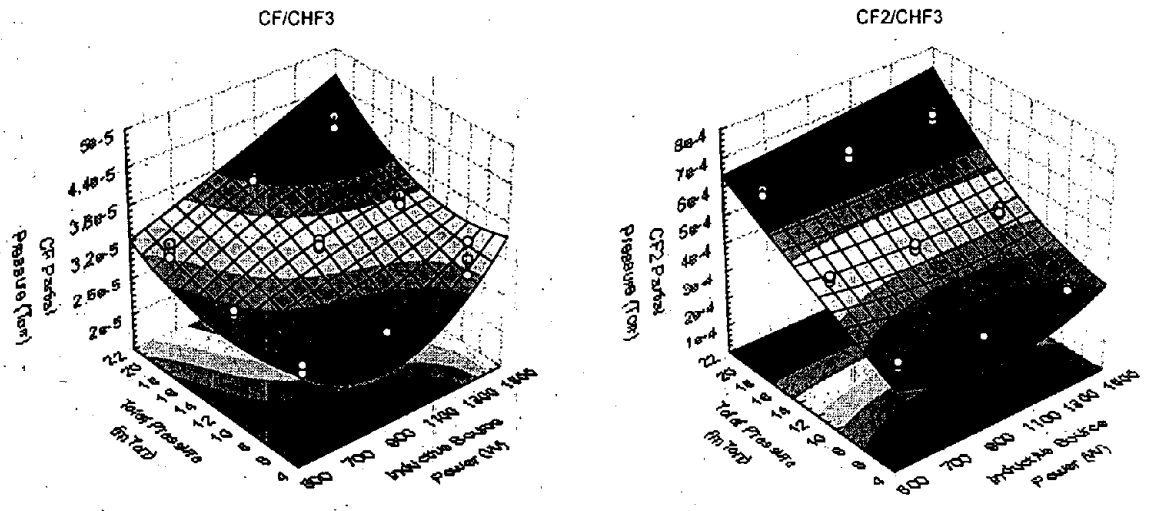

Figure 1 CF and CF_2 densities in a CHF_3 discharge in the SUNY-Albany reactor as a function of pressure and source power.

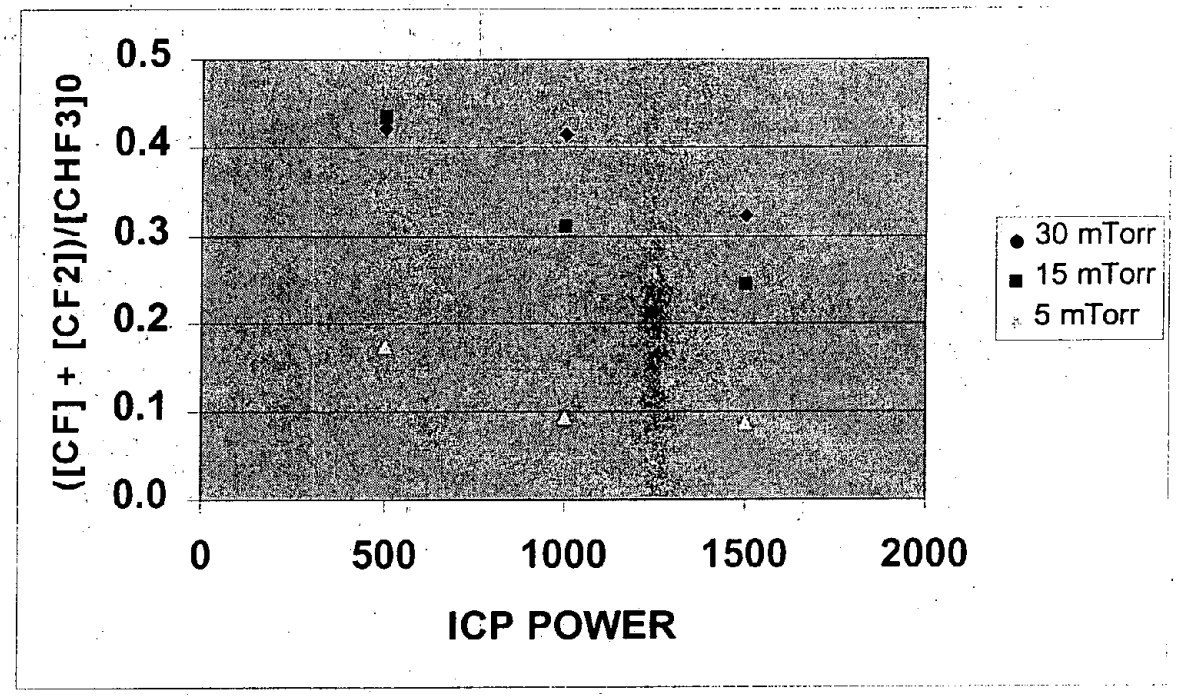

Figure 2 Plot of the ratio of the sum of the CF and CF_2 concentrations to that of CHF_3 as a function of ICP power for pressures of 5 to 15 mTorr.

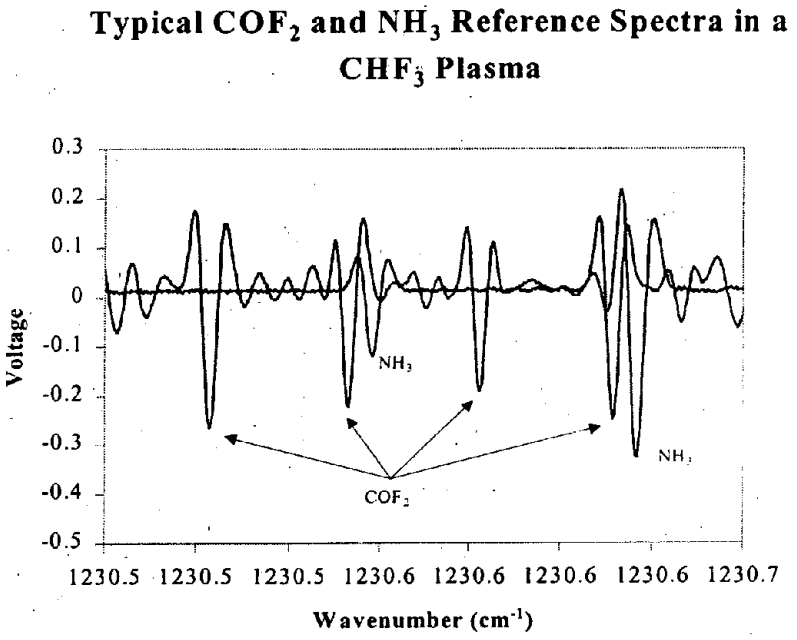

Figure 3 COF_2 absorption lines detected in CHF_3 plasma discharges in the SUNY-Albany reactor.

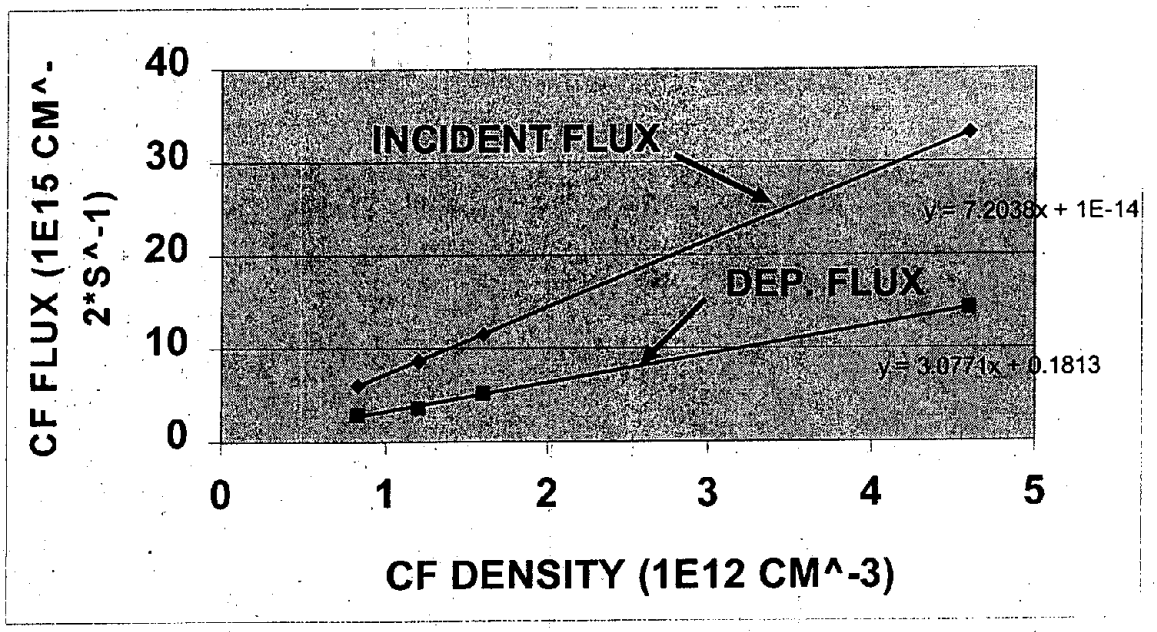

Figure 4 Comparison of the incident CF flux with the deposition flux inferred from [CF] measurements and the model described in the text.

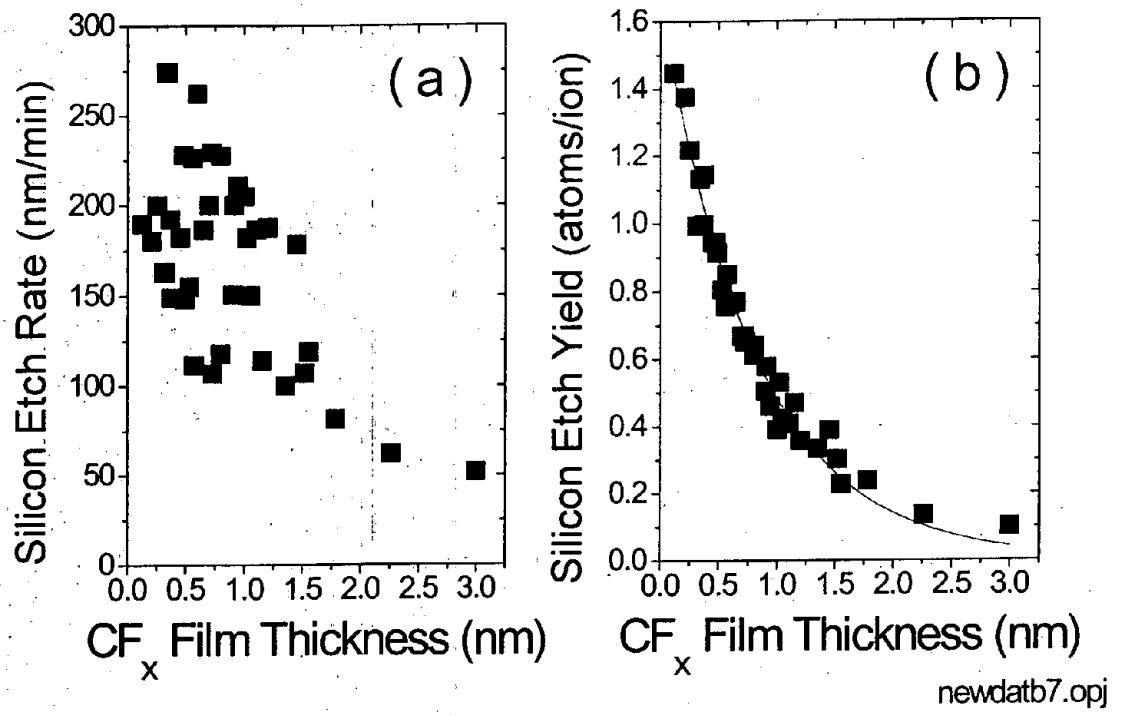

Fig. 5: (a) Silicon etch rates measured in C_2F_6 plasma for a variety of conditions (6-20 mTorr operating pressure, 10 - 40 sccm gas flow, and 600 - 1400 W inductive power) at -100 V self-bias as a function of the steady-state fluorocarbon film thickness measured for the same conditions. (b) The corresponding etch yields for the same conditions as a function of fluorocarbon film thickness.

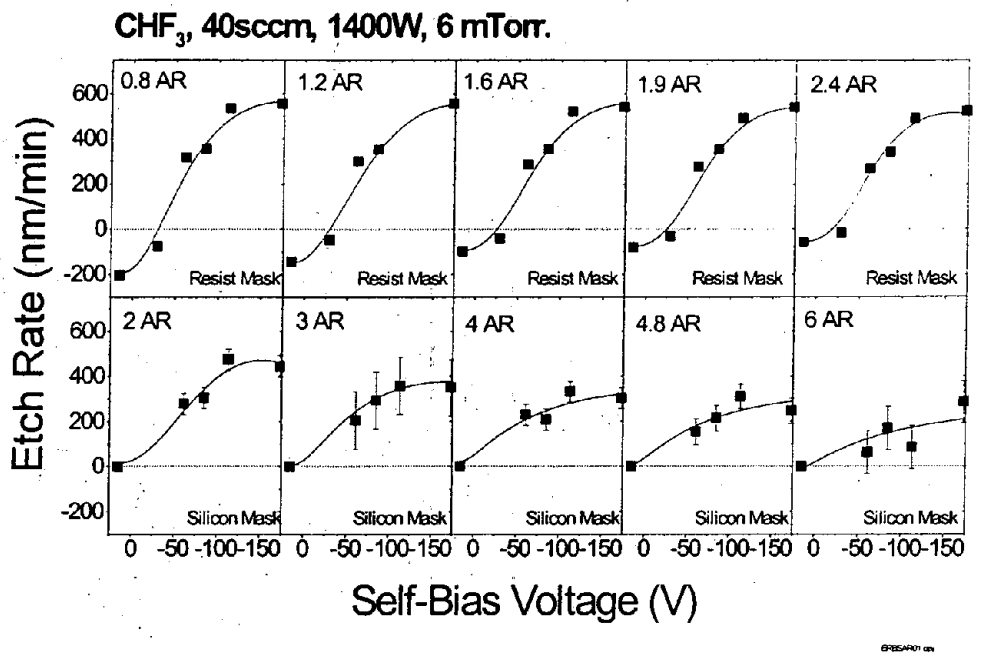

Figure 6 SiO_2 etch rate dependence on feature aspect ratio as a function of self-bias voltage.

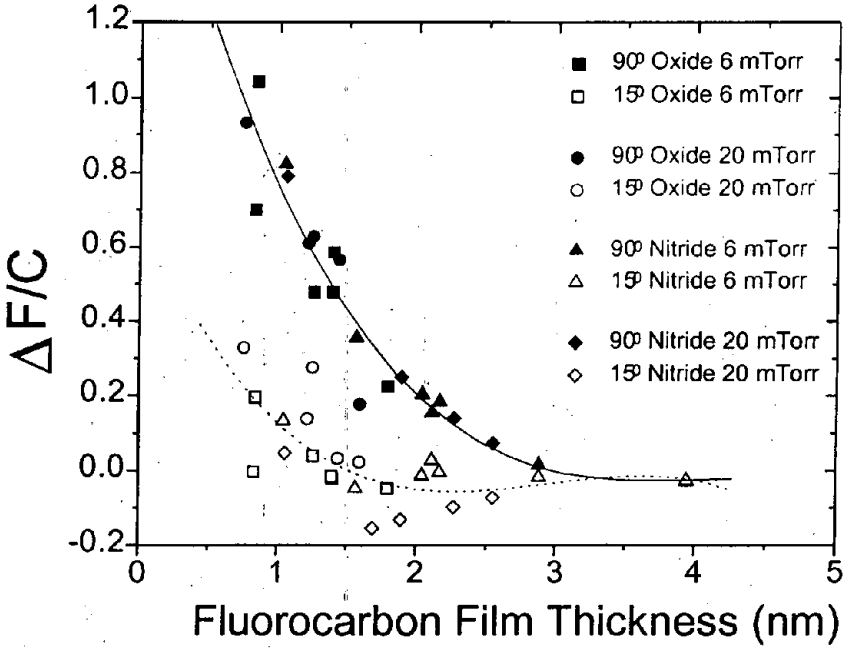

Figure 7: The difference between the fluorine to carbon ratios determined from F(1s)/C(1s) and C(1s) only, as a function of fluorocarbon film thickness.

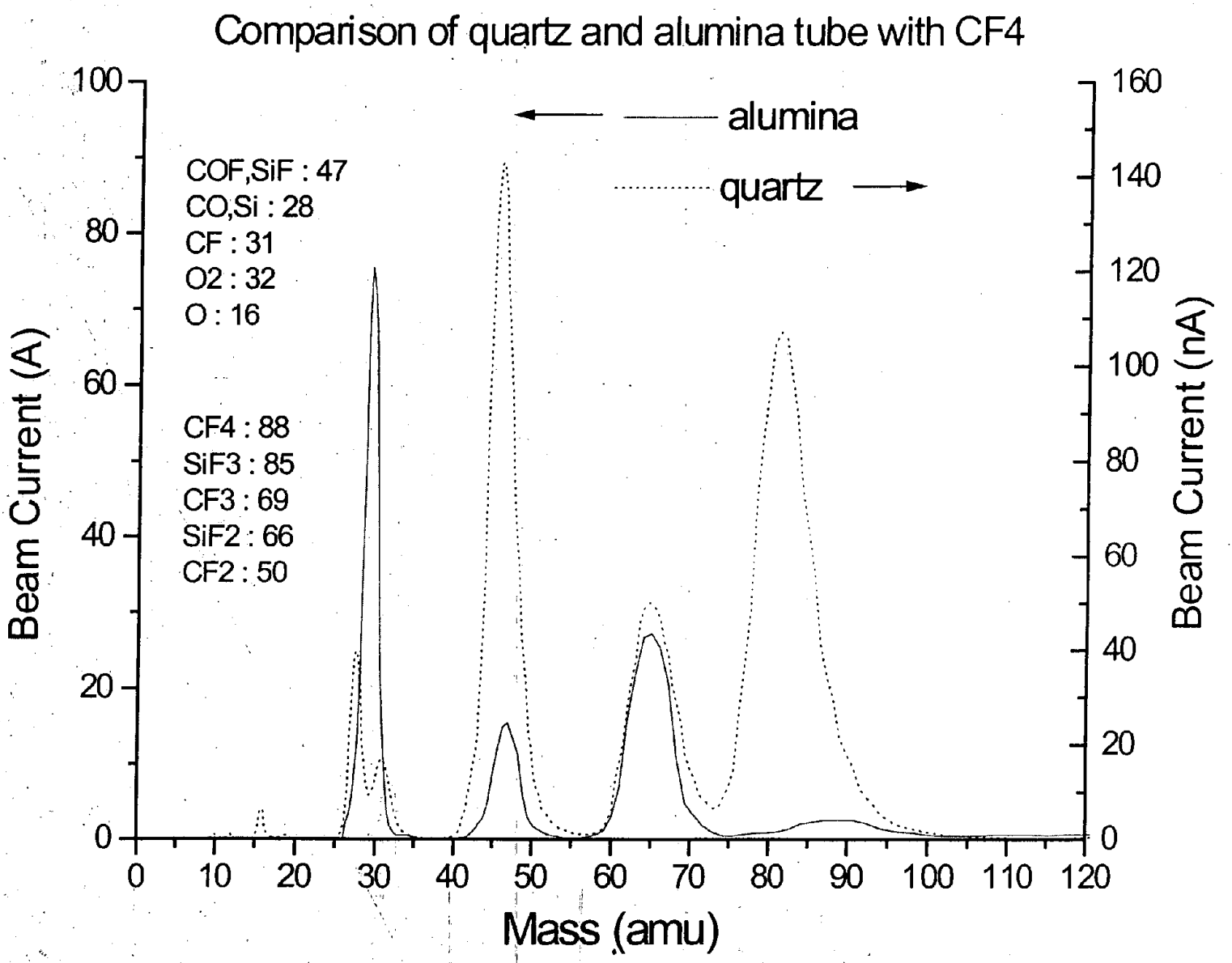

Figure 8 Comparison of the ion currents measured at the sample position versus mass for CF_4 discharges using a quartz liner or an aluminum liner of the ECR ion source.